Optimal transport of ultracold atoms in the non-adiabatic regime

A. Couvert, T. Kawalec, G. Reinaudi, David Guery-Odelin

▶ **To cite this version:**

A. Couvert, T. Kawalec, G. Reinaudi, David Guery-Odelin. Optimal transport of ultracold atoms in the non-adiabatic regime. 2007. hal-00168928v1

HAL Id: hal-00168928

https://hal.science/hal-00168928v1

Preprint submitted on 30 Aug 2007 (v1), last revised 15 Sep 2008 (v3)

HAL is a multi-disciplinary open access archive for the deposit and dissemination of scientific research documents, whether they are published or not. The documents may come from teaching and research institutions in France or abroad, or from public or private research centers.

L'archive ouverte pluridisciplinaire **HAL**, est destinée au dépôt et à la diffusion de documents scientifiques de niveau recherche, publiés ou non, émanant des établissements d'enseignement et de recherche français ou étrangers, des laboratoires publics ou privés.

Optimal transport of ultracold atoms in the non-adiabatic regime

A. Couvert, T. Kawalec, G. Reinaudi and D. Guéry-Odelin
Laboratoire Kastler Brossel, 24 rue Lhomond, F-75231 Paris Cedex 05, France*
(Dated: August 30, 2007)

We report on the transport of ultracold atoms with optical tweezers in the non-adiabatic regime i.e. on a time scale on the order of the oscillation period. To quantitatively interpret our data, we provide a fruitful analogy between the transport and the Fraunhofer diffraction of an object having a transmittance with the same shape as the one of the velocity profile imposed on center of the trap. The damping of the Kohn's mode due to the non-linear mixing turns out to be reminiscent of the effect of a finite coherence source for its optical counterpart.

PACS numbers: 32.80.Pj,39.25.+k,42.50.Vk

hal-00168928, version 1 - 30 Aug 2007

The controlled transport of ultracold atoms is crucial for the development of experiments in atomic physics. It renders possible to deliver cold atoms in a region free of the laser beams and coils of the magneto-optical trap (MOT), allowing a better optical and mechanical access. It also opens new perspectives for probing a surface or any material structure, and for loading atoms in optical lattices, or for positioning atoms in a high-Q optical cavity [1, 2]. In addition it renders possible a new generation of experimental setups where ultracold clouds of atoms would be delivered on demand on a variety of different experimental platforms separated by macroscopic distances. This is standard for charged particles and energetic neutral particles, it has also been recently accomplished with ultracold atoms by moving slowly optical tweezers [3]. Transport of cold packets of atoms is also of importance as a step towards the continuous production of a Bose-Einstein condensate [4, 5].

Magnetic transport has been demonstrated in macroscopic traps by moving mechanically a pair of coils [6, 7] or by using a set of coils with time-varying currents [8]. Those traps use a three-dimensional quadrupole configuration with a vanishing field at the center. The corresponding linear potential rapidly yields non-linear mixing resulting in a heating of the sample if the trap displacement is not performed in the adiabatic limit for which the duration of the transport is long with respect to the typical oscillation period of the trapped atoms. Alternatively one can resort to transport with Ioffe-Pritchard traps which have a harmonic bottom shape [5, 9, 10, 11], with optical tweezers as recently demonstrated on Bose condensed clouds [4] or with 1-D optical lattices [12, 13].

So far, the transport of atoms has been investigated only in the adiabatic regime. The issue of an optimal transport beyond this limit has been addressed numerically for ions in Paul traps [14]. In this article, we report on the transport of a cold atom cloud in the non-adiabatic regime with a high degree of control by means of optical tweezers. We also demonstrate how a fruitful analogy with optics permits to work out a new picture of the transport yielding a simple interpretation of our data and providing new methods for optimization.

The shape of the moving potential used to transport the atoms has a crucial role. The harmonic potential is of particular interest since the center of mass motion or otherwise stated the Kohn's mode is not coupled to the other degrees of freedom, and this is true both in presence and absence of interactions between atoms and both for classical and quantum physics.

We begin with a simple one-dimensional analytical model that provides a good quantitative understanding of the physics of the center of mass motion of a packet of atoms transported by a moving harmonic potential. We consider an atomic packet initially at rest in a harmonic trap of angular frequency ω_0, and with a r.m.s. size Δx. The trap position is given by the position of its center $x_c(t)$. For an atom of mass m, the imposed movement of the trap can be considered as an extra force whose expression is $-m\ddot{x}_c(t)$ in the frame attached to the trap.

According to Newton's law, the time dependent position $x(t)$ of the center of mass obeys the relation:

$$x(t) = x_c(t) + \frac{1}{\omega_0}\int_0^t dt' \sin[\omega_0(t'-t)]\ddot{x}_c(t') \ . \qquad (1)$$

After transporting the atoms from a point A to a point B (see Fig. 1.a) in a finite time T, the center of mass may oscillate. The amplitude $\mathcal{A}$ of this oscillatory motion is readily inferred from Eq. (1), and corresponds to the Fourier transform of the velocity profile of the trap's center position:

$$\mathcal{A}(T,\omega_0) = |\mathcal{F}[\dot{x}_c](\omega_0)| \ , \qquad (2)$$

with $\mathcal{F}[f] = \int_{-\infty}^{+\infty} f(t)e^{-i\omega t}\,dt$.

The simplest way to transport the packet of atoms from a point A to a point B separated by a distance d is to accelerate at a constant rate a during a time τ and to decelerate at the opposite rate $-a$ during the same time, yielding a Λ velocity profile (see Fig. 1.a). The parameters d, a and τ are then linked by the relation $a\tau^2 = d$. The resulting final amplitude, plotted on Fig. 1.b, is deduced from Eq. (2): $\mathcal{A}(2\tau,\omega_0) = d.\mathrm{sinc}^2(\omega_0\tau/2)$, where the $\mathrm{sinc}(x)$ function is defined as $\sin(x)/x$. Its zeros as a function of time are the optimal transport durations

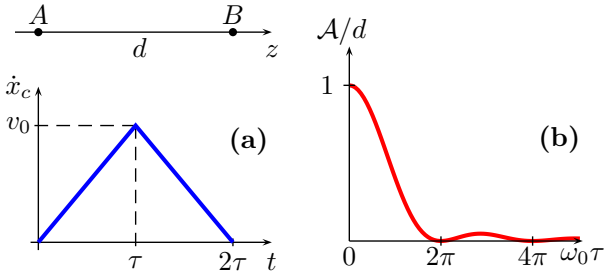

FIG. 1: (Color online). (a) We consider the transport of a packet of atoms from a point A to a point B with a Λ-shape profile for the velocity imposed on the center of the harmonic trapping potential. (b) The residual amplitude $\mathcal{A}$ oscillation of the center of mass after transport is the Fourier transform of the velocity profile. An optimal transport ($\mathcal{A} = 0$) can be performed within a time on the order of the period of oscillation $T_0 = 2\pi/\omega_0$.

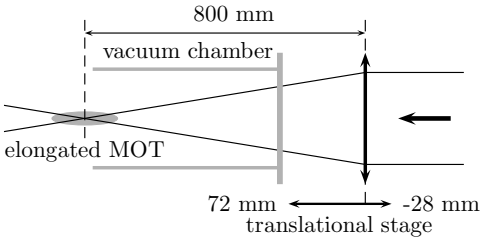

FIG. 2: Sketch of the main part of the experimental setup (not to scale) — see text.

$2\tau_n = 2nT_0$, where $T_0 = 2\pi/\omega_0$ is the period of oscillation of the trap, and n a non zero integer. They correspond to a transport without residual dipole mode excitation. It is worth noticing that $\mathcal{A}^2$ is nothing but the far field Fraunhofer diffraction pattern of an object with a transmittance given by a Λ-shape similar to the one of the velocity profile. We find, for this specific example, that it is possible to move optimally a packet of atoms on any distance d on a time as short as twice the oscillation period. This is to be contrasted with the transport in the adiabatic limit ($\omega_0\tau \gg 1$) for which the transport's duration is long compared to T_0.

A reasonable definition of an "adiabatic criterium" for the transport of a packet is that the amplitude of the center of mass motion remains small with respect to its size Δx, or otherwise stated that the maximum acceleration of the trap during the whole transport remains small with respect to the acceleration scale $\omega_0^2\Delta x$. We point out that the result obtained above is valid for arbitrary values of the acceleration $a = d/\tau^2$, the movement can thus be deeply in the non-adiabatic regime.

The Fourier transform formulation of the transport allows for many enlightening analogies. For instance, the minimum duration of an optimal transport, independently of the specific shape of the velocity profile, is necessarily larger than the period of oscillation T_0. Our example of a Λ velocity profile is already close to this limit. As another example, a more elaborated sequence where a packet of atoms is transported from a point A to a point B, and then from B to C with a similar velocity profile can be regarded as a Young's two-slit experiment.

For the experimental implementation, we have used optical tweezers generated by a focused laser beam (see Fig. 2). We use an Ytterbium fiber laser (IPG LASER, model YLR-300-LP) with a central wavelength of 1072 nm and a FWHM linewidth of 4 nm. The wavelength of the laser is larger than the atomic resonance wavelength of 780.24 nm of the Rubidium 87 atoms, and thus, atoms are attracted to the region of maximum intensity [15]. The laser beam intensity is controlled and stabilized to better than 0.1% in a power range up to 100 W. The beam is expanded with a two-lens telescope to a waist of about 6 mm, and focused inside the vacuum chamber by a lens with a 802 mm focal length (see Fig. 2). This final lens is mounted on a translation stage (Newport linear motor stage, model XMS100), allowing one to move the optical tweezers longitudinally on a 100 mm range with an absolute repeatability on the order of a few hundreds of nm. The waist is on the order of 50 ± 4 μm, corresponding to a Rayleigh length of 10.0 ± 0.5 mm, and a potential depth $U_{\rm depth}$ of 3 mK at 80 W.

The optical tweezers are loaded from an elongated MOT. The cigar-shape of the MOT results from the two-dimensional magnetic gradients: $(0, 5, -5)$ G/cm. The MOT, loaded from a Zeeman slower, has a capture rate on the order of 2×10^{10} atoms/s. To maximize the loading of atoms into the dipole beam, the optical tweezers are superimposed on the MOT along its long axis. In addition, we favour the selection of atoms in the hyperfine low level $5S_{1/2}, F = 1$ by removing the repump light in the overlapping region similarly to the dark MOT technique [16].

The dipole trapping beam is turned on at a power of 80 W during the 500 ms loading time of the MOT. Then, we increase the MOT detuning in 5 ms from -3Γ to -7.7Γ, Γ being the natural frequency width of the excited state. This procedure improves significantly the optical tweezers loading. The magnetic field and repumping light are switched off and a 1 ms polarization stage is applied to optically pump atoms to the $F = 1$ ground sublevel. Finally all the MOT beams are turned off. The number of atoms in the optical tweezers is as high as 3×10^7 corresponding to a peak atomic density of 5×10^{12} at/cm^3. These numbers are measured 50 ms after switching off the MOT beams, so a first evaporation has already occurred on this timescale since the collision rate is larger than 500 s^{-1}.

The atomic packet is further cooled down by forced evaporation achieved by lowering the beam power i.e. the trap depth. Two different cooling schemes were used. In

the first one, referred to scheme 1, the initial trapping beam power is lowered in two linear ramps by a factor of 23 within 600 ms. The final atomic cloud temperature is 27 ± 1.0 μK. In scheme 2 the beam power is decreased in four linear ramps by a factor of 170 within 3300 ms, resulting in a 3.7 ± 0.5 μK temperature of the atomic packet. To render the trapping potential as harmonic as possible one has to maximize the parameter $\eta = U_{\rm depth}/k_B T$. This is achieved by adiabatically increasing the power P after evaporation. In this process, $U_{\rm depth}$ scales as P, while the temperature T increases at a lower rate ($\propto P^{1/2}$) resulting in an increase of $\eta \propto P^{1/2}$. The trapping beam power after this re-compression and before transporting the atoms reaches 37 W (resp. 42 W). The η parameter is thus equal to 13 (resp. 50) for scheme 1 (resp. 2). These two different schemes permit to identify the conditions under which a non-adiabatic transport can be performed when the anharmonicities of the trapping potential are not completely negligible.

The radial angular frequencies of the recompressed trap were inferred from a parametric heating experiment: $\omega_x = 2\pi \cdot (1600 \pm 100)$ Hz and $\omega_y = 2\pi \cdot (2100 \pm 100)$ Hz. The longitudinal angular frequency was measured by examining the cloud dipole mode oscillations. We find $\omega_0 = 51 \pm 2$ rd/s (resp. $\omega_0 = 56 \pm 2$ rd/s) for the scheme 1 (resp. 2). The initial number of atoms and cloud temperature before the transport is 2.1×10^6 at 160 ± 11 μK (resp. 5.7×10^6 at 43 ± 2 μK) for the scheme 1 (resp. 2), corresponding to a r.m.s. size $\Delta x = (k_B T/m\omega_0^2)^{1/2} \simeq 2.4$ mm (resp. 1.2 mm).

The transport experiment has been carried out in a single vacuum chamber. We consequently imposed a "round trip" displacement of the optical tweezers going from the MOT location A to a point B placed 22.5 mm from it along the beam direction, and back to A (see Fig. 3a). The transport's duration is 4τ and the velocity profile has a "$\Lambda - V$ shape". It corresponds to a Young's two slit like experiment with a time separation of 2τ. The different transport durations were obtained by varying the acceleration a from 0.2 to 3.3 m.s^{-2}, ensuring a transport in the non-adiabatic regime.

The transport is accompanied by a heating of the cloud. For scheme 1 (resp. 2), we find a relative increase of temperature of 10% (resp. 75%) after a transport duration longer than one period of oscillation ($\omega_0 \tau \geq 2\pi$). The cloud at the lower temperature is obviously more sensitive to heating mechanism such as transverse shaking of the cloud, or photon scattering. The latter effect remains relatively small for both schemes, while the former could be reduced by using an air bearing translation stage instead of a standard linear rail guided translation stage.

For each amplitude measurement $\mathcal{A}(4\tau, \omega_0)$, we chose an acceleration value a, or equivalently a transport duration $\tau = (d/a)^{1/2}$, and we measure the center of mass oscillations after the transport by recording a set of typically 30 images separated from one another by 10 ms. The images are acquired using a standard absorption imaging technique on a CCD camera. Since the imaging process is destructive, the whole experimental sequence has to be redone for each picture.

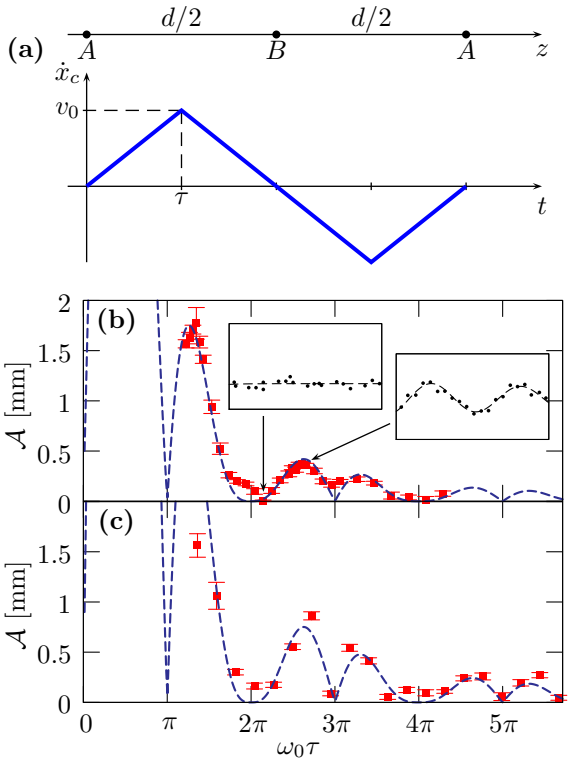

FIG. 3: (Color online) (a) Back and forth transport from A to B and B to A ($d = 45$ mm) with the velocity profile imposed to the trap. (b) (resp. (c)) The measured amplitude $\mathcal{A}$ of the center of mass dipole oscillation for the conditions of scheme 1 (resp. 2), see text. Inset of (b): Typical data of the position of the center mass as a function of time. The dashed line is the theoretical prediction of Eq. (3) with the measured angular frequency ω_0 of the trap.

The position of the center of mass of the cloud as a function of time is inferred from a 2D Gaussian fit . We deduce the amplitude of oscillation of the center of mass by fitting this position data (see insets of Fig. 3b). The theoretical amplitude of oscillation after the transport is readily obtained from Eq. (2):

$$\mathcal{A}(4\tau, \omega_0) = 2d.\mathrm{sinc}^2(\omega_0\tau/2)|\sin(\omega_0\tau)| \ . \qquad (3)$$

One recognizes the contribution of a Λ or V shape transmittance in the first two factors. The last factor simply accounts for "interferences" between the Λ and V velocity profiles. We distinguish in the forthcoming discussion two kinds of zeros: the even ones originating from the "diffraction" factor ($\omega_0\tau = 2p\pi$, p being an integer) and an extra set of odd zeros due to the "interference" factor only ($\omega_0\tau = (2p+1)\pi$, p being an integer).

The comparison of our experimental data with the the-

ory is made with only one adjustable parameter: a global multiplying factor for the amplitude. Indeed the angular frequency ω_0 is directly measured by the dipole mode analysis. We find a very good agreement between our data and formula (3) (see Figs. 3b and c). The shown error bars reflect the fitting uncertainties.

We observe a non-vanishing amplitude of the dipole mode for the first observed odd zero ($\omega_0\tau = 3\pi$) for the data of scheme 1 by contrast to the data of scheme 2. We interpret this phenomenon by taking into account the non-linear mixing resulting from anharmonicities of the trapping potential. This effect is stronger for scheme 1 which is characterized by a smaller η parameter compared to the one of the scheme 2. The non-linear mixing mimics a damping that turns out to be analogous to the effect of the finite spatial or temporal coherence of a source illuminating the two slits of a Young's experiment.

For a transportation made of a succession of similar velocities profiles, we have worked out the results of the simplest damping model with a friction like force ($-2m\gamma\dot{x}$). For the $\Lambda - V$ profile, the formula for the pseudo-amplitude $\tilde{\mathcal{A}}$ of the dipole mode reads

$$\tilde{\mathcal{A}} = \mathcal{A}_0 . \frac{\Omega^2}{\omega_0^2} \frac{|1 - \mathcal{V}_1 \cos(\Omega\tau)|}{(\Omega\tau/2)^2} . |1 - \mathcal{V}_2 \cos(2\Omega\tau)|^{1/2} \ , \quad (4)$$

with $\Omega = (\omega_0^2 - \lambda^2)^{1/2}$ and the visibility factors $\mathcal{V}_n \simeq 1 - n^2(\gamma\tau)^2/2$ in the regime where $\gamma\tau \ll 1$. We thus obtain two kinds of minima for the dipole mode amplitude affected by the damping in a different manner: The ones that result from "interferences" factor and that are sensitive to the damping of the center of mass oscillation at the first order ($\min(\tilde{\mathcal{A}}) \simeq 2\sqrt{2}\mathcal{A}_0\gamma\tau$) and the ones of the "diffraction pattern" factor that are nearly "decoherence-free" ($\min(\tilde{\mathcal{A}}) \simeq \mathcal{A}_0\gamma^3\tau^3/2$) and thus preferred for a robust optimized transportation. This refined analysis yields a visibility $\mathcal{V}_2$ of 85% (resp. 100%) for scheme 1 (resp. 2). In addition the curvature of those minima is important (see Fig. 3b and c). Indeed, a flat minimum enhances the robustness of the transport against fluctuations of the movement duration or the trap frequencies.

The same qualitative features for the zeros of the amplitude of the dipole mode remain valid for a $\Lambda - \Lambda$ velocity profile. In addition, we emphasize that a vanishing amplitude can always be recovered by shaping the velocity profile to compensate for the damping effect.

The theoretical framework presented in this article to analyze our data on the transport of atoms using optical tweezers allows to work out a more elaborated shape yielding very flat minima. Apodization techniques, commonly used in optics, can be transposed to the velocity profile to remove the secondary peaks of the amplitude of the motion after the transport. Velocity profiles derived in this manner would permit one to transport or stop the optical tweezers in a very optimized fashion for the transport of atoms even in presence of a residual damping.

We thank J. Dalibard, A. Ridinger and T. Lahaye for careful reading of the manuscript. Support for this research came from the Délégation Générale pour l'Armement (DGA), the Institut Francilien de Recherche sur les Atomes Froids (IFRAF) and the Plan-Pluri Formation (PPF) devoted to the manipulation of cold atoms by powerful lasers. G. R. acknowledges support from the DGA.

[*] Unité de Recherche de l'Ecole Normale Supérieure et de l'Université Pierre et Marie Curie, associée au CNRS.

[1] J. A. Sauer, K. M. Fortier, M. S. Chang, C. D. Hamley, and M. S. Chapman, Phys. Rev. A **69**, 051804(R) (2004).
[2] Y. Colombe, T. Steinmetz, G. Dubois, F. Linke, D. Hunger and J. Reichel, arXiv:0706.1390.
[3] T. L. Gustavson, A. P. Chikkatur, A. E. Leanhardt, A. Görlitz, S. Gupta, D. E. Pritchard, and W. Ketterle, Phys. Rev. Lett. **88**, 020401 (2002); A. E. Leanhardt, A. P. Chikkatur, D. Kielpinski, Y. Shin, T. L. Gustavson, W. Ketterle, and D. E. Pritchard, *ibid* **89**, 040401 (2002).
[4] A. P. Chikkatur, Y. Shin, A. E. Leanhardt, D. Kielpinski, E. Tsikata, T. L. Gustavson, D. E. Pritchard, and W. Ketterle, Science **296**, 2193 (2002).
[5] T. Lahaye, G. Reinaudi, Z. Wang, A. Couvert and D. Guéry-Odelin, Phys. Rev. A **74**, 033622 (2006).
[6] H. J. Lewandowski , D. M. Harber, D. L. Whitaker and E. A. Cornell, J. Low Temp. Phys. **132**, 309 (2003).
[7] K. Nakagawa, Y. Suzuki, M. Horikoshi and J. B. Kim, Appl. Phys. B, **81**, 791 (2005).
[8] M. Greiner, I. Bloch, T. W. Hänsch and T. Esslinger, Phys. Rev. A **63**, 031401 (2001).
[9] W. Hänsel, J. Reichel, P. Hommelhoff and T. W. Hänsch, Phys. Rev. Lett. **86**, 608 (2001).
[10] P. Hommelhoff, W. Hänsel, T. Steinmetz, T. W. Hänsch and J. Reichel, New J. Phys. **7**, 3 (2005).
[11] A. Günther, M. Kemmler, S. Kraft, C. J. Vale, C. Zimmermann and J. Fortágh, Phys. Rev. A **71**, 063619 (2005).
[12] S. Kuhr, W. Alt, D. Schrader, M. Müller, V. Gomer and D. Meschede, Science **293**, 278 (2001).
[13] S. Schmid, G. Thalhammer, K. Winkler, F. Lang and J. H. Denschlag, New J. Phys. **8**, 159 (2006).
[14] S. Schulz, U. Poschinger, K. Singer and F. Schmidt-Kaller, Fortschr. Phys. **54**, 648 (2006).
[15] R. Grimm, M. Weidemüller, and Yu.B. Ovchinnikov Adv. At. Mol. Opt. Phys. **42**, 95 (2000).
[16] W. Ketterle, K. B. Davis, M. A. Joffe, A. Martin and D. E. Pritchard, Phys. Rev. Lett. **70**, 2253 (1993).